Journal of Power Sources 195 (2010) 6207–6211

Contents lists available at ScienceDirect

Journal of Power Sources

journal homepage: www.elsevier.com/locate/jpowsour

Electrolyte properties of 1-alkyl-2,3,5-trimethylpyrazolium cation-based room-temperature ionic liquids for lithium secondary batteries

Shiro Seki [a,*], Takeshi Kobayashi [a], Nobuyuki Serizawa [a], Yo Kobayashi [a], Katsuhito Takei [a], Hajime Miyashiro [a], Kikuko Hayamizu [b], Seiji Tsuzuki [b], Takushi Mitsugi [c], Yasuhiro Umebayashi [c], Masayoshi Watanabe [d]

[a] Materials Science Research Laboratory, Central Research Institute of Electric Power Industry (CRIEPI), 2-11-1, Iwado-kita, Komae, Tokyo 201-8511, Japan
[b] National Institute of Advanced Industrial Science and Technology (AIST), Tsukuba Center 5, Tsukuba, Ibaraki 305-8565, Japan
[c] Department of Chemistry, Faculty of Science, Kyushu University, Hakozaki, Higashi-ku, Fukuoka 812-8581, Japan
[d] Department of Chemistry and Biotechnology, Yokohama National University, 79-5 Tokiwadai, Hodogaya-ku, Yokohama, Kanagawa, Japan

ARTICLE INFO

Article history:
Received 30 September 2009
Received in revised form 27 October 2009
Accepted 29 October 2009
Available online 10 November 2009

Keywords:
Lithium secondary battery
Room-temperature ionic liquid
Physicochemical properties
Electrode
Interface

ABSTRACT

The physicochemical and electrochemical properties of three 1-alkyl-2,3,5-trimethylpyrazolium cation-based room-temperature ionic liquids with various alkyl chain lengths were investigated. The temperature dependences of density, viscosity, and ionic conductivity were obtained by precise measurements. Electrolyte properties of these room-temperature ionic liquids were also examined from the viewpoint of their uses in lithium secondary batteries ([$LiCoO_2$ positive electrode|electrolyte|lithium metal negative electrode]). It was found that the alkyl chain length affects the charge–discharge performances of cells.

1. Introduction

Room-temperature ionic liquids (room-temperature molten salts, RTILs) are liquid salts consisting of only cations (positive ions) and anions (negative ions) and have desirable and interesting properties, for example, low flammability and low volatility (negligible vapor pressure), high ionic conductivity, and thermal and electrochemical stability [1]. RTILs have unlimited possibilities through synthetic chemistry by varying the combination of cations and anions and they also have various promising physicochemical properties and can be used in task-specific applications. For example, RTILs have been attracting attentions as safe lithium secondary battery electrolytes for use in high-performance, large-scale energy storage devices, such as electric power load-leveling systems for customer usages and natural power storage systems (PV, wind power) [2–4]. However, the relatively high viscosities of common RTILs (e.g., imidazolium and quaternary ammonium cation systems), which are attributed to the strong interactions (e.g., coulombic forces) and intramolecular (e.g., rotational) energies, are serious issues. In this study, we studied three different 1-alkyl-2,3,5-trimethylpyrazolium cation-based RTILs (alkyl: ethyl, propyl, and butyl), which retain relatively low viscosity with increasing cationic molecular weight. The physicochemical (density, viscosity, ionic conductivity) and electrochemical (battery performances) properties were investigated.

2. Experimental

2.1. Samples

RTILs based on 1-alkyl-2,3,5-trimethylpyrazolium bis (trifluoromethanesulfonyl) amide (purchased from Kanto Kagaku, synthesized by Japan Carlit) were used as the RTIL samples, and the chemical structures are shown in Fig. 1. The samples contained an ethyl (ETMP-TFSA, M_w: 419.36), propyl (PTMP-TFSA, M_w: 431.37) or butyl (BTMP-TFSA, M_w: 447.42) groups. The RTIL samples were dried in a vacuum chamber at 323 K for more than 48 h and stored in a dry argon-filled glove box ([O_2] < 0.4 ppm, [H_2O] < 0.1 ppm, Miwa Mfg. Co., Ltd.) before various measurements were performed.

2.2. Measurements of physical properties of RTILs

Density (ρ) and viscosity (η) measurements were performed using a thermoregulated Stabinger-type density/viscosity meter

* Corresponding author. Tel.: +81 3 3480 2111; fax: +81 3 3480 3401.
E-mail address: s-seki@criepi.denken.or.jp (S. Seki).

0378-7753/$ – see front matter © 2009 Elsevier B.V. All rights reserved.
doi:10.1016/j.jpowsour.2009.10.081

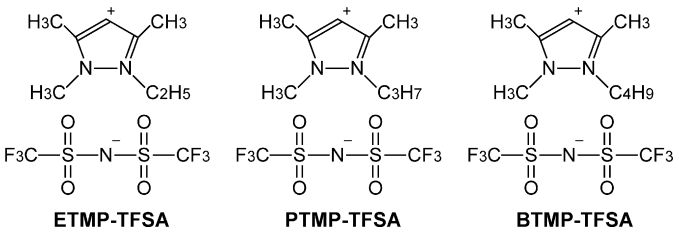

Fig. 1. Chemical structures of 1-alkyl-2,3,5-trimethylpyrazolium cation-based room-temperature ionic liquids (ETMP-TFSA, PTMP-TFSA, and BTMP-TFSA).

(SVM3000G2, Anton Paar). The temperature was controlled in the range of 80–10 °C while cooling. Ionic conductivity (σ) was measured on SUS/electrolyte/SUS hermetically closed cells and determined by the complex impedance method using an AC impedance analyzer (Princeton Applied Research, PARSTAT-2263, frequency region: 200 kHz–50 mHz, impressed voltage: 10 mV) at temperatures between 80 and −40 °C while cooling.

2.3. Preparation and evaluation of lithium secondary batteries using RTILs

Lithium secondary battery characteristics were investigated using [$LiCoO_2$ positive electrode|RTIL electrolyte|lithium metal negative electrode] cells. The positive electrode sheet was composed of $LiCoO_2$ (85 wt.%) as the active material, acetylene black (9 wt.%, Denka) as an electrically conductive additive, and PVDF (6 wt.%, Kureha Chemical) as a binder polymer. These constitutive materials were thoroughly agitated together in a homogenizer with *N*-methylpyrrolidone (NMP). The obtained positive electrode paste was uniformly applied onto an aluminum current collector using an automatic applicator. After drying the applied paste, the positive electrode sheet was compressed using a roll-press machine to increase packing density and to improve electrical conductivity (electrode thickness after roll-pressing: 15 μm, electrode loading: 3 mg cm^{-2}). The positive electrode sheet, separator, RTIL–Li-TFSA binary electrolyte (Li-TFSA concentration: 0.32 mol kg^{-1}), and lithium metal negative electrode were encapsulated into 2032-type coin cells. To ensure complete penetration of the electrolyte into the high-density pressed positive electrode sheet, the prepared battery was aged at 60 °C for more than 18 h. Then, charge–discharge tests were performed on the cells at 3.0–4.2 V with a current density of 0.05 mA cm^{-2} (constant current charge–constant current discharge). AC impedance measurements were performed at every cycle in the charged state (frequency region: 200 kHz–50 mHz, impressed voltage: 10 mV, Princeton Applied Research VMP2/Z). The cycle number dependences of the impedance spectra, which were obtained using the fitting program ZSimpWin will be discussed below. All measurements were performed at 30 °C.

3. Results and discussion

3.1. Bulk properties of RTILs

Fig. 2 shows the temperature dependences of density (ρ) for ETMP-TFSA, PTMP-TFSA, and BTMP-TFSA. The densities of the pyrazolium cation-based RTILs decreased in the order ETMP-TFSA > PTMP-TFSA > BTMP-TFSA in the measured temperature range. For example, the densities at 30 °C ($\rho_{30\,°C}$) were 1.454 (ETMP-TFSA), 1.421 (PTMP-TFSA), and 1.388 g cm^{-3} (BTMP-TFSA). The densities decreased with the alkyl chain length, similarly to in the widely reported 1,3-alkyl imidazolium cation-based systems [5]. Generally, in a narrow range of temperatures, ρ (g cm^{-3}) can be

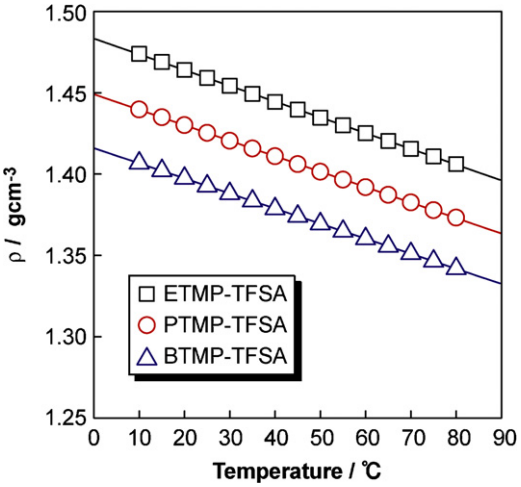

Fig. 2. Temperature dependences of density (ρ) for 1-alkyl-2,3,5-trimethylpyrazolium cation-based room-temperature ionic liquids upon cooling (80–10 °C).

Table 1
Density equation ($\rho = b - aT$) parameters and molar concentration at 30 °C (M_{30}) for ETMP-TFSA, PTMP-TFSA, and BTMP-TFSA.

Ionic liquids	a ($\times 10^{-4}$ g cm^{-3} K^{-1})	b (g cm^{-3})	M_{30} ($\times 10^{-3}$ mol cm^{-3})
ETMP-TFSA	9.691	1.483	3.468
PTMP-TFSA	9.514	1.449	3.293
BTMP-TFSA	9.269	1.415	3.102

expressed as follows:

$$\rho = b - aT, \quad (1)$$

where a, b, and T are the coefficient of volume expansion (g cm^{-3} K^{-1}), the density at 0 K (g cm^{-3}), and temperature (K), respectively. In the present system a strong linear relationship ($r > 0.9999$) with temperature was obtained for all RTILs. The best-fit parameters of Eq. (1) are summarized in Table 1. The molar concentration (at 30 °C; M_{30}/mol cm^{-3}) and the degree of expansion of pyrazolium cation-based RTILs also decreased with the alkyl chain length of the RTILs as well as ρ.

Fig. 3 shows the temperature dependences of viscosity (η) for ETMP-TFSA, PTMP-TFSA, and BTMP-TFSA. The values of η for ETMP-TFSA, PTMP-TFSA, and BTMP-TFSA at 30 °C were 68, 62,

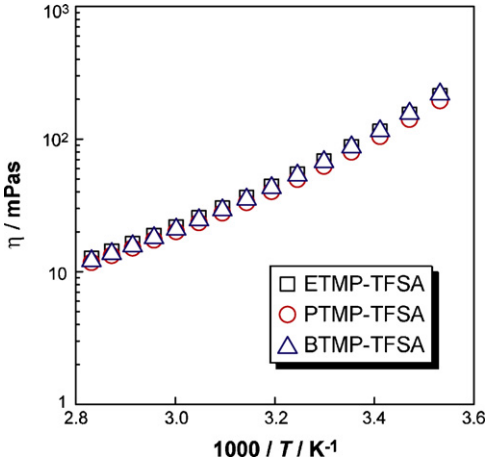

Fig. 3. Temperature dependences of viscosity (η) for 1-alkyl-2,3,5-trimethylpyrazolium cation-based room-temperature ionic liquids upon cooling (80–10 °C).

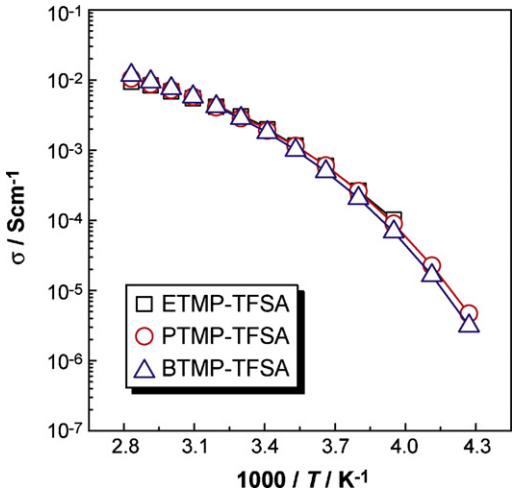

Fig. 4. Temperature dependences of ionic conductivity (σ) for 1-alkyl-2,3,5-trimethylpyrazolium cation-based room-temperature ionic liquids upon cooling (80 to −40 °C).

and 67 mPa s, respectively, and independent of alkyl chain length. Fig. 4 gives the temperature dependences of ionic conductivity (σ) for ETMP-TFSA, PTMP-TFSA, and BTMP-TFSA. The values of σ for ETMP-TFSA, PTMP-TFSA, and BTMP-TFSA at 30 °C were 3.0, 2.8, and 2.8 mS cm^{-1}, respectively. On the other hand, common imidazolium cation-based RTILs have been reported significant effects of length of alkyl chain on physicochemical properties, and the reported values of η and σ at 30 °C varied with alkyl chain length (C_2mim-TFSA: 27 mPa s, 11 mS cm^{-1}, C_4mim-TFSA: 40 mPa s, 4.6 mS cm^{-1}) [5]. The causes of the relatively high values of η and low values of σ for three RTILs are thought arising from their week coulombic forces (intermolecular), high internal mobility (intramolecular), and bulky molecular shape. In all RTIL systems (e.g., imidazolium, quaternary ammonium, pyrazolium, etc.), coulombic forces should be affected by ionic size, for example, the alkyl chain length. In this study, the viscosity and ionic conductivity of pyrazolium cation-based RTILs are shown to be less affected by ionic sizes than those of imidazolium cation-based RTILs. The intramolecular mobility might one of the important factors for the pyrazolium cation-based RTILs to determine the viscosity and ionic conductivity.

3.2. Battery electrolyte properties of RTILs

To investigate the relationships between alkyl chain length in the pyrazolium cation and actual lithium secondary battery performances, charge–discharge tests were performed using [$LiCoO_2$|lithium metal] cells. Fig. 5(a) shows the cycle number dependence of the charge–discharge profiles of the [$LiCoO_2$ positive electrode|ETMP-TFSA/Li-TFSA electrolyte|lithium metal negative electrode] cell at 303 K (voltage region: 4.2–3.0 V, current density: 50 μA cm^{-2} = C/8). A relatively high initial (1st cycle) coulombic efficiency of 97% was observed with stable charge/discharge operation. The changes in the average charge and discharge voltage with the cycle number were extremely low [average charge voltage: 3.99 V (1st), 4.00 V (50th), 4.00 V (100th), 4.01 V (150th), average discharge voltage: 3.92 V (1st), 3.90 V (50th), 3.89 V (100th), 3.89 V (150th)], and no significant changes in polarization or degradation were observed. Fig. 5(b) shows the cycle number dependences of the discharge capacities of the [$LiCoO_2$ positive electrode|RTIL/Li-TFSA electrolyte|lithium metal negative electrode] cells for the three RTILs. The initial discharge capacities of the prepared cell for the three RTIL systems were approximately 130–135 mA h g^{-1}, which is close to the theoretical capacity for Li_xCoO_2 ($0.5 < x < 1$;

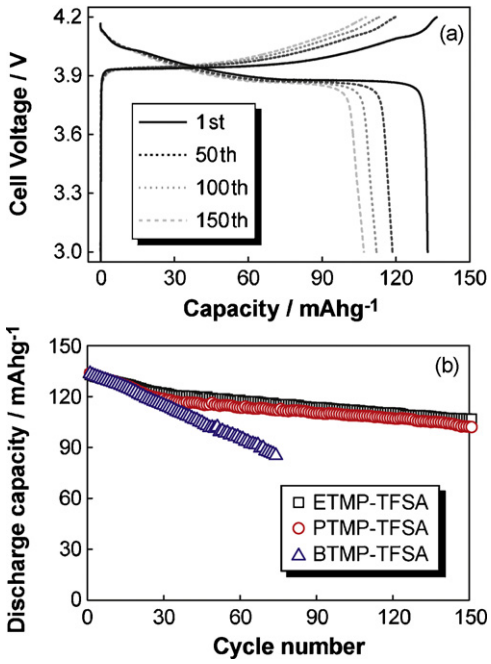

Fig. 5. Charge–discharge profiles of the [$LiCoO_2$ positive electrode|RTIL/Li-TFSA|lithium metal negative electrode] cells (a) in 1st, 50th, 100th, and 150th cycles and (b) relationship between cycle number and discharge capacity of cells with various 1-alkyl-2,3,5-trimethylpyrazolium cation-based RTILs.

operation voltage: 3.0–4.2 V). The cycle performances of the prepared cells improved with decreasing alkyl chain length in the pyrazolium cation, particularly when the alkyl chain is shorter than butyl. Pyrazolium cation-based RTILs exhibited the opposite result to that for imidazolium cation-based RTILs where the longer alkyl chain RTILs gave the better performances [6]. Moreover, the improvement of reversibility was confirmed upon introducing the electron-releasing substituted group at the second position of the imidazolium cation. In the case of the imidazolium cation, it is expected that the high reactivity of the hydrogen at the second position leads to a low electrochemical stability. Pyrazolium cation does not have the activated position owing to the methylation, and therefore high charge/discharge reversibilities were achieved. The average rate of discharge capacity degradation for the ETMP, PTMP, and BTMP systems was 0.15, 0.16, and 0.65 mA h g^{-1}/cycle, respectively, a ratio of approximately 1:1:4. To estimate the degradation factors of the prepared cells with numbers of charge/discharge cycles, we investigated the changes in resistance inside the cells by AC impedance analysis. Fig. 6 shows the typical impedance spectrum for the [$LiCoO_2$ positive electrode|RTIL/Li-TFSA electrolyte|lithium metal negative electrode] cell in the charged state (4.2 V, electrolyte: ETMP-TFSA/Li-TFSA, at 100 cycles) (Table 2). Two semicircular arcs were observed in all cycles and for the all RTILs. On the basis of the response frequency (related to the time constant of the kinetics for each electrode) obtained in a previous study, it is concluded that the impedance components are the electrolyte bulk, lithium metal/electrolyte interface, and $LiCoO_2$/electrolyte interface in decreasing frequency [7]. Therefore, we assumed the equivalent circuit (a series circuit of R_{bulk}, $R_{lithium}Q_{lithium}$, and $R_{LiCoO_2}Q_{LiCoO_2}$; R and Q are the resistance and a constant phase element; incomplete capacitance element, respectively), depicted in Fig. 6. Using the assumed equivalent circuit, the fitting of the impedance spectrum was carried out. Calculated values were consistent with measured values within the accuracy of the measurements. The charge–discharge cycle number dependences of R_{bulk}, $R_{lithium}$, and R_{LiCoO_2} are shown in Fig. 7(a), (b), and (c), respectively. For all RTIL

Table 2
Impedance fitting parameters of the [$LiCoO_2$ positive electrode|RTIL/Li-TFSA|lithium metal negative electrode] cells at 4.2 V after 100 charge/discharge cycles using equivalent circuit (shown in Fig. 6).

	R_{bulk}	$R_{lithium}$	R_{LiCoO_2}	$Q_{lithium}$	Q_{LiCoO_2}
Resistance ($\Omega\,cm^2$)	17.3	164.0	64.9	–	–
Capacitance (Fcm^{-2})	–	–	–	2.60×10^{-5}	2.07×10^{-2}

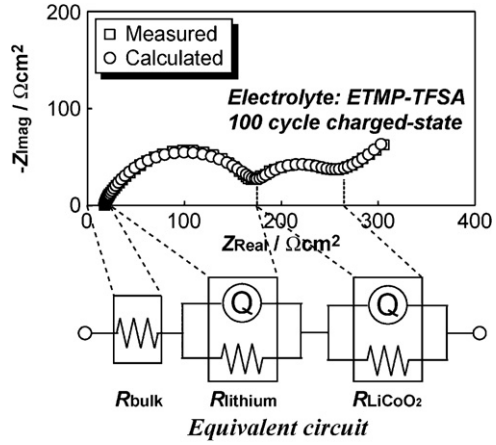

Fig. 6. Measured and calculated impedance plots of [$LiCoO_2$|ETMP-TFSA electrolyte|lithium metal] cell at 4.2 V after 100 charge/discharge cycles, and the assumed equivalent circuit of the measured cell.

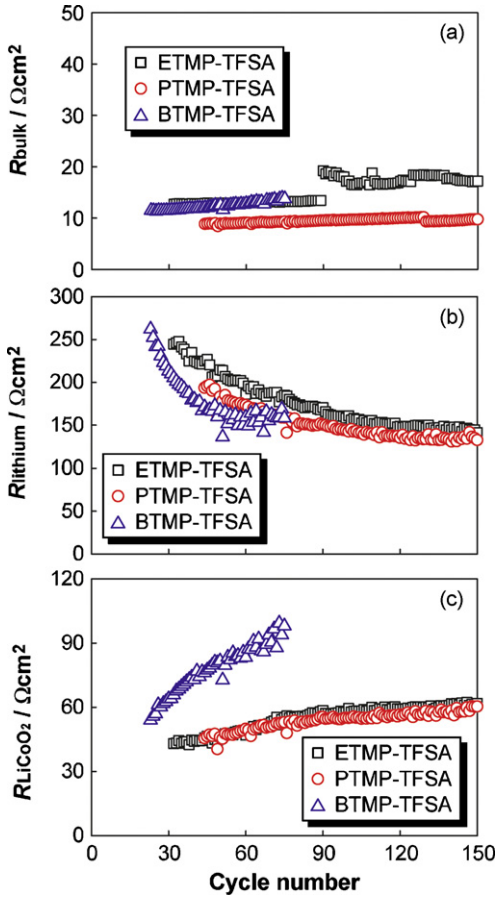

Fig. 7. Cycle number dependences of electrolyte bulk resistance (R_{bulk}) (a), electrolyte/lithium metal interfacial resistance ($R_{lithium}$) (b), and electrolyte/$LiCoO_2$ interfacial resistance (R_{LiCoO_2}) (c) of [$LiCoO_2$|RTIL|lithium metal] cells with various 1-alkyl-2,3,5-trimethylpyrazolium cation-based RTILs at 4.2 V.

systems, no significant cycle-dependent changes were observed in R_{bulk} up to 150 cycles. No noticeable degradation of the bulk RTIL/Li-TFSA electrolytes and separators (electrolyte layer) was confirmed. $R_{lithium}$ decreased with increasing numbers of charge–discharge cycles up to about 60 cycles then stabilized at approximately 150 $\Omega\,cm^2$. The dissolution and deposition of lithium ($Li \leftrightarrow Li^+ + e^-$) repeatedly occur at the lithium metal/electrolyte interface with each charge–discharge operation. As a result, the surface area of the metallic lithium electrode increases, which might have caused by the decrease of the convergence. In contrast, R_{LiCoO_2} increased linearly with cycle number, and the ratio of the rate of increase was approximately (ETMP:PTMP:BTMP) = 1:1:4, which agreed with the behavior of discharge capacity deterioration. From the impedance analysis, the dominant cause of cell degradation with charge–discharge cycling is the $LiCoO_2$/electrolyte interface. Moreover, cathodic stability may be influenced by the alkyl chain length of pyrazolium cations. Generally, molecular size affects the viscosity and ionic conductivity for common RTILs (e.g., those with imidazolium and quaternary ammonium cations). In the pyrazolium cation-based RTILs, intramolecular mobility including pyrazolium ring can contribute electrochemical stability through the formation of many conformational isomers owing to the low entropy. Spectroscopic (IR, Raman) and computational studies based on solution chemistry are expected to provide more detailed information, which will allow us to determine the relationships between electrochemical (microscopic) and physicochemical (macroscopic) phenomena.

4. Conclusions

The physicochemical and electrolytic properties of 1-alkyl-2,3,5-trimethylpyrazolium cation-based room-temperature ionic liquids (alkyl: ethyl, propyl, butyl) were investigated, focusing on their use in lithium secondary batteries. The results are summarized as follows:

1. The density of pyrazolium cation-based RTILs decreased with increasing length of the alkyl chain, similar to the trend for well-known imidazolium cation-based RTILs. On the other hand, viscosity and ionic conductivity were not affected by the change in alkyl chain length.
2. The charge–discharge cycle performances of [$LiCoO_2$|RTIL/Li-TFSA electrolyte|lithium metal] cells were improved with decreasing alkyl chain length in the pyrazolium cation ring, particularly when the alkyl chain is less than butyl. For example, a high charge–discharge reversibilities (over 100 mA h g^{-1}) after 150 cycles were achieved when the alkyl chains were ethyl and propyl groups (ETMP and PTMP) and reversibility was reduced in BTMP.

Acknowledgement

The authors acknowledge Mr. Daizo Kameoka (Electric Power Engineering Systems Co., Ltd.) for technical support in the experiments.

References

[1] M. Armand, F. Endres, D.R. MacFarlane, H. Ohno, B. Scrosati, Nat. Mater. 8 (2009) 621.
[2] H. Sakaebe, H. Matsumoto, Electrochem. Commun. 5 (2003) 594.
[3] M. Ishikawa, T. Sugimoto, M. Kikuta, E. Ishiko, M. Kono, J. Power Sources 162 (2006) 658.
[4] S. Seki, Y. Kobayashi, H. Miyashiro, Y. Ohno, A. Usami, Y. Mita, N. Kihira, M. Watanabe, N. Terada, J. Phys. Chem. B 110 (2006) 10228.
[5] H. Tokuda, K. Hayamizu, K. Ishii, M.A.B.H. Susan, M. Watanabe, J. Phys. Chem. B 109 (2005) 6103.
[6] S. Seki, Y. Mita, H. Tokuda, Y. Ohno, Y. Kobayashi, A. Usami, M. Watanabe, N. Terada, H. Miyashiro, Electrochem. Solid-State Lett. 10 (2007) A237.
[7] S. Seki, Y. Ohno, H. Miyashiro, Y. Kobayashi, A. Usami, Y. Mita, N. Terada, K. Hayamizu, S. Tsuzuki, M. Watanabe, J. Electrochem. Soc. 155 (2008) A421.